16 Apr 1992

Design and Development of a Superconducting Induction Motor

Terry Bowness

DESIGN AND DEVELOPMENT OF A SUPERCONDUCTING INDUCTION MOTOR

Terry Bowness
Dept. of Physics
University of Missouri-Rolla

ABSTRACT

The discovery of high-T_c superconductors has led to the development of a number of experimental superconducting motors. This report documents the design, construction, and methods of evaluating the performance of an induction motor with a high-T_c superconducting rotor. While others have utilized the Meissner effect, our superconducting motor works due to Lenz's law. In theory such a device will act as an induction motor only during start-up, after which its behavior is more like that of a synchronous machine. With a one-pole copper squirrel cage providing start-up torque two high-T_c discs encased in the rotor core act to bring the machine to synchronous speed.

INTRODUCTION

There has been a great deal of effort directed toward the development of higher-efficiency electrical machines. The idea of using superconducting components to achieve such goals is not new, but with the discovery of high-T_c Type II superconductors in 1986 interest in this area has been rekindled. Prior to this time the only known superconductors required liquid helium cooling systems which for many applications is simply too expensive. One of the chief advantages of the new materials is the relatively low cost of cooling with liquid nitrogen (LN_2). At this time, however, use of high-T_c superconductors is hindered by the limited number of physical forms in which they can be manufactured.

This report describes the development of a two-phase induction motor with a superconducting rotor, part of an ongoing undergraduate research effort at UMR. Such a device will in theory operate as an induction motor only during start-up, after which its behavior will be more like that of a synchronous machine.[1] In other words the small amount of slip characteristic of conventional induction motors goes to zero when the rotor reaches superconductivity. The rotor consists of two high-T_c $YBa_2Cu_3O_x$ discs surrounded by a single-pole copper squirrel cage, all encased in a laminated iron core. Increased efficiency as a result of the elimination of rotor power losses and hysteresis should be seen by comparing the operation of the same rotor with copper discs instead of the superconducting ones.

The theory of operation will be covered first in order to explain why the slip goes to zero and what the expected torque and power outputs should be. The design and implementation of the stator, power supply, rotor, and test apparatus are then described. Finally, an analysis of experimental data is included and compared to theoretical predictions.

THEORY

We will first consider the operation of a classical two-phase induction motor. The motor can be divided into two parts, the stator and the rotor (see Figure 1). The stator consists of four electromagnets placed 90 mechanical degrees apart. These magnets are powered by two a.c. voltage sources that are 90 electrical degrees out of phase, creating a rotating magnetic field. The rotor, centered between all four pole faces, is illustrated in Figures 2 and 3. As shown in these figures the rotor consists of a metallic "squirrel cage," generally copper, embedded in a

laminated iron core. The iron serves as a low-reluctance pathway through which the magnetic flux created by the stator may travel.

Even though each bar of the squirrel cage is connected to the same two end plates the rotor may be thought of as being composed of several discrete rectangular loops or poles. This is shown in Figure 4. The rotating **B** (magnetic) field created by the stator causes a change in the amount of flux passing through each loop. This induces a current in the conductor which works to oppose the change in flux (Lenz's law). The current loop creates a magnetic moment which, due to interaction with the rotating stator field, causes a torque about the axis of the rotor. See Appendix One for a derivation of the torque equation. The flux, Φ, linking one loop is given by the dot product of **B** and the area vector **A**, or $BA\cos\Theta$. If the **B** field rotates with constant angular velocity, w, then the torque on one pole will vary sinusoidally. The minimum number of poles required to create a constant torque is three; since there are two bars per pole most squirrel cages have at least six bars.

An important concept in induction motors is that of slip. The rotor of a conventional induction motor will never reach synchronous speed, w_s, i.e. the speed at which the **B** field rotates. Consider what would happen if somehow we did force the rotor to spin at w_s. At this point the current in the conductors of the squirrel cage would be zero since the flux linked by each loop would remain constant. With no current there is no torque, and with no torque the rotor will begin to slow down due to frictional forces. As the rotational velocity decreases, however, Φ begins to vary sinusoidally, inducing current and torque on the bars of the squirrel cage. There will be a speed at which this torque will balance out the frictional torque. The rotor will continue at that rate until the motor is connected to a load.[2] Slip is defined as the per unit difference between w_s and angular velocity of the rotor, w_r:

$$s = (w_s - w_r)/w_s \tag{1}$$

A common circuit model for the induction motor, the Steinmetz model, relates voltage and current characteristics to those of a transformer.[3] Shown in Figure 5a with its Thevinin equivalent circuit in Figure 5b, it is the basis for all the following equations. The output torque is given by[4]

$$\tau = \frac{2I_2^2 r_2(1-s)/s - P_{rot}}{w_s(1-s)} \tag{2}$$

where P_{rot} is the power loss due to air and rotational friction. The value for maximum torque will be[5]

$$\tau_{max} = 2\frac{\frac{V_i^2}{w_s}\left[\frac{jX_m}{r_1 + j(x_1 + X_m)}\right]^2 \frac{r_2}{s}}{\left(R_1 + \frac{r_2}{s}\right)^2 + (X_1 + x_2)^2} \tag{3}$$

which holds true for any value of r_2, however, for a given r_2 τ_{max} will occur at a particular slip:[6]

$$s_m = \frac{r_2}{\sqrt{R_1^2 + (X_1 + x_2)^2}} \qquad (4)$$

The mechanical power output and efficiency are simply

$$P_{out} = \tau \cdot w_s \cdot (1 - s) \qquad (5)$$

$$\epsilon = P_{out}/P_{in} \qquad (6)$$

with

$$P_{in} = V_1 \cdot I_1 \cdot \cos\Theta_p \qquad (7)$$

where Θ_p is the angle of the phasor impedance seen looking into the input terminals.

It is readily seen that these relationships fail to adequately describe the induction motor with a superconducting rotor. Because the rotor is superconducting its resistance and the slip, r_2 and s, are both zero. Substituting zero for the values of r_2 and s, the above equation for torque becomes the undefined quantity 0/0. Note, however, that for $r_2 = 0$ the slip at which τ_{max} occurs is zero, so it appears that there will indeed be no slip, however, a new expression is need to predict what the torque will be. At the time of this writing we have not completely derived this expression.

As described previously, the primary difference between the conventional and superconducting induction motors is in the rotor; all other components are essentially the same. A motor proposed by Brechna and Kronig employs two squirrel cages, one made from low-grade copper and the other from a superconductor.[7] Theirs was conceived before the advent of high-T_c type II materials, thus a cage of low-T_c niobium, zirconium, or niobium-tin alloy would present no problem other than the system for cooling with liquid helium. High-T_c superconductors are ceramic and therefore very brittle, however, and do not lend themselves readily to being milled or machined. A previous group at UMR working on this project attempted to have a squirrel cage cast from $YBa_2Cu_3O_x$ with no success.[8] For this reason our superconductors were left as discs and encased in an iron core with axes perpendicular to the axis of the rotor shaft as illustrated in Figure 6.

A one-pole copper squirrel cage provides torque during start-up. There can be no start-up torque with an r_2 of zero. This is demonstrated in equation (2) by letting $s = 1$ and $r_2 = 0$. Thus the copper provides the necessary resistance to accelerate the rotor from a standstill. As the rotor achieves minimum slip it is cooled to liquid nitrogen temperatures ($\approx$77 K). Synchronous speed is reached following a transient response as the rotor goes superconducting and the copper ceases to provide torque.[9] It was mentioned earlier that three poles are needed to produce a steady torque on the shaft, but our rotor has only one. Since a steady acceleration of the motor during start-up is not critical in such a small laboratory motor is was decided that one pole would suffice for experimental purposes.

To understand how the machine operates at synchronous speed a brief look at high-T_c

superconductors is in order. Superconductivity is dependent on not only temperature but also on magnetic field strength and current density within the sample. This is shown in Figure 7. Note that there are not one but two critical magnetic field strengths, H_{c1} and H_{c2}. Above H_{c2} there is no superconductivity. Below H_{c1} the sample will behave as a perfect superconductor in which all lines of magnetic flux are expelled from the sample.[10] This complete expulsion of flux from the interior of the superconducting sample is known as the Meissner effect.[11] In the region between H_{c1} and H_{c2} magnetic flux penetrates the sample as flux vortices. The sample remains a superconductor with zero resistance. Any attempt to change the flux density will result in increased vortex density within the sample.[12] If each flux vortex is pinned to imperfections in the sample the average field strength cannot change and a surface current is induced according to Lenz's law. If the flux vortices can easily move in and out of the superconducting sample, the eddy currents induced in the normal metal at the core of each vortex constitute a loss mechanism which creates an a.c. resistance. Strongly pinned flux vortices are necessary for lossless a.c. superconductor operation.[13]

Efforts to create a high-T_c superconducting motor in recent years have not been based on the above principles. Consider a sample cooled in the presence of a gradient field of strength greater then zero but below H_{c1}. Eddy currents acting to expel the internal flux will in turn produce a force on the sample. This idea was used by researchers at Sanyo in a simple Meissner motor in which the superconductors were mounted on the rotor.[14] Another group at the University of Arkansas, Fayetteville, employed superconductors as levitation bearings. Small magnets were mounted at the ends of the rotor shaft, which was levitated above high-T_c discs to achieve low bearing friction.[15]

Our superconducting induction motor does not make use of the Meissner effect, rather, it operates by Lenz's law. As explained previously the rotor is brought to within a few percent of synchronous speed before being cooled. The magnitude of the **H** field, H_0, will be between H_{c1} and H_{c2}. Initially the stator field will still rotate faster than the rotor, so from the point of view of the superconducting discs there is a changing flux density. Again, this induces eddy currents in the sample (Lenz's law) which act to maintain the internal flux density at B_o. These currents create a magnetic dipole which is stationary relative to the rotor itself, unlike the dipoles of the conventional motor which rotate slightly faster than the rotor. This fixed dipole enables the rotor to "catch up" with the stator field, transforming the device into a synchronous machine. Bringing the machine up to speed in this manner is quite similar to the way large industrial synchronous motors are started from a stand-still using auxiliary induction motors.[16]

DESIGN OF THE MOTOR AND TEST APPARATUS

The stator used in this research was designed and constructed by Beckman, Peacher, and Thornborrow, a previous UMR physics group working on this project.[17] Figure 7 illustrates its layout. The four poles are identical electromagnets of 500 turns each whose laminated iron cores measure 1.5" square in cross section. Power is provided to the stator with a two-phase function generator and a power amplifier. The function generator outputs two sinusoids with adjustable relative phase. Setting the phase for 90° will produce a **B** field rotating in one direction while setting it to 270° will rotate it the other way.

Our rotor design expands on that of Beckman et. al., shown in Figure 9, with the

addition of a one-pole squirrel cage and a cylindrical iron core. The squirrel cage provides starting torque while the iron core greatly reduces secondary leakage reactance, x_2. The result is the rotor shown in Figure 6.

A significant problem is created by the need to cool the rotor with liquid nitrogen. For the most efficient use of LN_2 it is best to insulate the rotor from the iron stator cores, which are moderate conductors of heat. To minimize leakage reactance x_2, however, the air gap between the rotor and stator needs to be made as small as possible. In the design by Brechna and Kronig the coolant, in their case liquid helium, is fed through a hollow rotor shaft to the rotor itself.[18] We opted instead to insulate the rotor in a foam-covered plastic container and simply pump LN_2 into the container (see Figure 10 for details). The flow of nitrogen is controlled by the power dissipated in a 30Ω resistor submerged in the large dewar. It was found that six to eight watts provides a flow of nitrogen sufficient to maintain superconductivity. This cooling system is advantageous over that of Brechna and Kronig in that it eliminates the need for a rotating seal on the end of the shaft, however it inevitably increases the width of the air gap.

Self-lubricated ball bearings are used to suspend the shaft. The biggest disadvantage to implementing this type of bearing is that they must be kept warm, preferably close to room temperature; rolling friction increases dramatically as the temperature of the lubricant is lowered. A 68Ω power resistor has been attached to each bearing with good thermal contact provided by silicon heat-sink compound. These resistors are inadequate when used alone, however, because of cold air escaping from the reservoir and blowing directly onto the bearings. For this reason two metal discs 1.5" in diameter with a .25" hole in the center are situated on the shaft just outside the reservoir. With these in place the two heaters work very well with about six watts supplied to each one.

To evaluate the performance of the superconducting induction motor it is necessary to measure the operating speed, the static torque, and the dynamic torque. A simple tachometer has been built which utilizes an interrupter module, illustrated in Figure 11. When the space between the arms of the module is unobstructed the unit outputs zero volts. If a solid object passes through it the output voltage goes to a positive d.c. value. As the rotor shaft turns the holes in the disc pass through the interrupter module, creating a series of short pulses which can be observed on an oscilloscope. Utilizing a frequency counter the frequency of the pulse train can be divided by the number of holes in the disc to obtain the rotor speed.

Measurement of the static torque, τ_s, is fairly simple. Figure 11 illustrates a means of performing this measurement. The spring constant, k, must be found first. With the spring attached to the shaft the motor is turned on and the distance, d, that the spring is stretched is found, which in turn will give the force F being exerted upon it. F is then multiplied by the radius of the rotor shaft, r, giving the value of τ_s.[19]

Finding τ_d, the dynamic torque, takes somewhat more effort. In Figure 12 the shaft is shown with a string wrapped around it a few times with one end tied to a mass and the other connected to a spring. The top of the spring is connected to a stationary object. Once the motor is running and the mass and spring are at fixed positions, the problem becomes one of statics. The frictional force, F_f, is equal to the force due to the spring minus the weight of the mass, W. τ_d is again the force tangent to the surface of the shaft times the shaft radius.

$$\tau_d = r \cdot (F_s - W) \quad (8)$$

EXPERIMENTAL RESULTS

The superconducting induction motor was tested with the rotor constructed by Beckman, Peacher, and Thornborrow. Maximum speed occurred when the stator field angular velocity was at or below 10 Hz although spinning of the rotor could be maintained with w_s as high as 40 Hz. While in theory there should have been no starting torque, the rotor did indeed start from a stand-still by itself when the stator field was at frequencies less than ten hertz. This can be attributed to the nature of the superconducting samples; these samples exhibit very little flux pinning, thus there was eddy current drag in the cores of the flux vortices. If the superconductors exhibited perfect flux pinning there would be no eddy current drag and therefore no net starting torque.[20]

Experimentation with a non-superconducting, one-pole rotor of dimensions similar to the new superconducting one indicated that the torque produced by our stator may be insufficient to overcome the new rotor's rather large moment of inertia. Unfortunately fabrication of the new rotor was not completed in time for it to be tested. If this research is continued it may be desirable to design and construct a smaller superconducting rotor.

CONCLUSIONS AND RECOMMENDATIONS

One of the most significant problems with our motor involved keeping the bearings warm. The ones used were self-lubricated ball bearings which became very lossy when the rotor was cooled. It was necessary to install baffles in addition to small heaters to reduce cooling by convection and conduction, respectively. It may therefore be worthwhile to look into alternative types of bearings, for example air bearings, which require no lubrication and operate with a minimal amount of friction.

There many improvements which can be made on our motor as well as a number of tests which have not yet been performed. The new rotor needs to be tested with superconducting discs that exhibit a high degree of flux pinning. It remains to be seen whether or not the motor will actually run at synchronous speed. Measurements of static and dynamic torque must be made. An expression for the torque on a superconducting disc in a rotating **B** field as a function of Θ should be developed. The resistance and reactance values of the Steinmetz circuit model could be determined from the blocked-rotor and no-load tests.[21] In general what is needed is more experimental data to determine exactly how the motor performs and how practical of a machine it really is.

ACKNOWLEDGEMENTS

Much of the knowledge and guidance behind this project has been patiently provided by Dr. Don M. Sparlin of the University of Missouri-Rolla Physics Department. Thanks also to Mr. Russell Summers for the design and construction of our stator power supply and interrupter module and to Mr. Charles McWhorter for his work in machining several of the vital motor components.

REFERENCES

1. H. Brechna and H. Kronig, "Three-phase induction motor with superconducting cage winding," IEEE Transaction on Magnetics **15(1)**, 715 (1979).
2. George McPherson and Robert D Laramore, An introduction to electrical machine and Transformers (John Wiley and Sons, New York, 1981), 2nd ed., Chap. 4, pp. 243-245.
3. McPherson and Laramore, 247.
4. McPherson and Laramore, 258.
5. McPherson and Laramore, 265.
6. McPherson and Laramore, 267.
7. Brechna and Kronig, 715.
8. D.M. Sparlin, University of Missouri-Rolla Physics Dept., private communication.
9. Brechna and Kronig, 715.
10. Raymond A. Serway, Superconducting supplement for physics for scientists and engineers (Saunders College Publishing, Chicago, 1988), 2nd ed., p. 16.
11. Serway, 10.
12. Serway, 15-17.
13. D.M. Sparlin, private communication.
14. A. Takeoka, A. Ishikawa, M. Suzuki, K. Niki, and Y. Kuwano, "Meissner motor using high-T_c ceramic superconductors," IEEE Transactions on Magnetics **25(2)**, 2511-2514 (1989).
15. David E. Weeks, "High-T_c superconducting levitation motor with laser commutator," Review of Scientific Instruments **61(1)**, 195-197 (1990).
16. McPherson and Laramore, Chap. 2, pp. 93-94.
17. A. Beckman, J.F. Peacher, and C. Thornborrow, UMR Physics Dept., "An induction motor using a high critical temperature superconductor motor."
18. Brechna and Kronig, 715.
19. Beckman, Peacher, and Thornborrow, 13.
20. D.M. Sparlin, private communication.
21. McPherson and Laramore, 276-281.

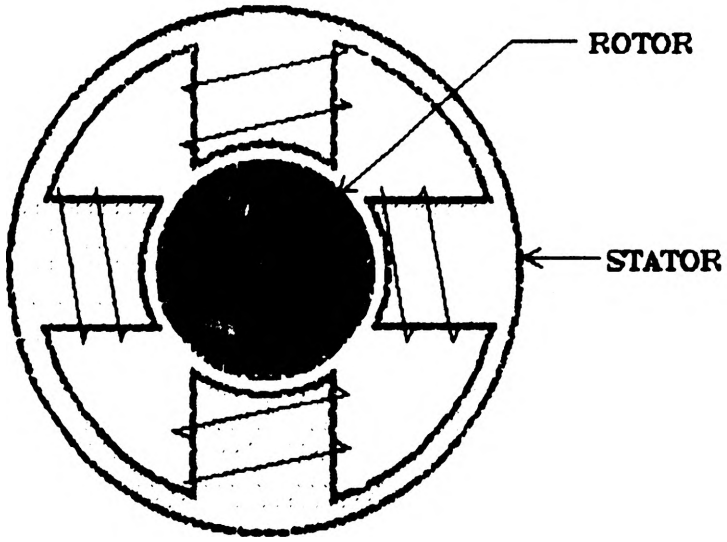

FIGURE 1--CONVENTIONAL INDUCTION MOTOR

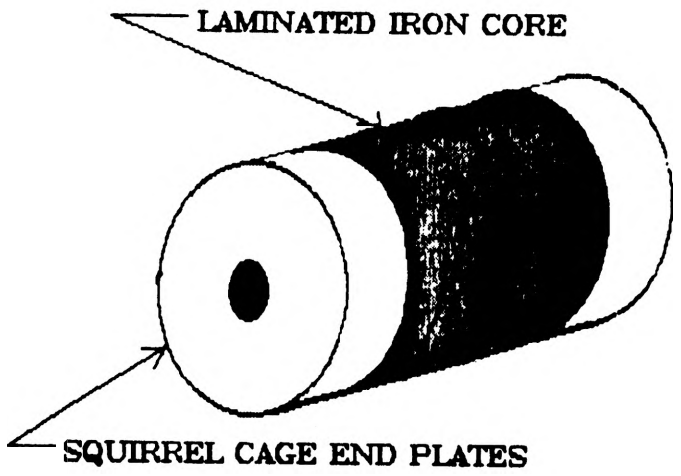

FIGURE 2--TYPICAL ROTOR

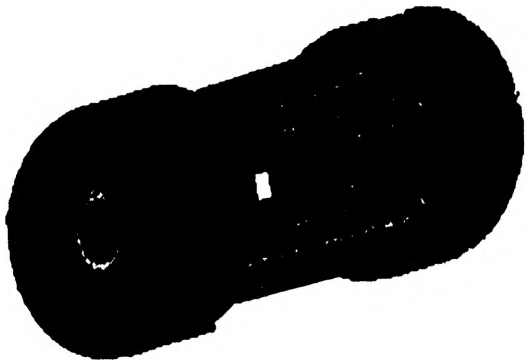

FIGURE 3--ROTOR SQUIRREL CAGE

ILLUSTRATION OF SQUIRREL CAGE AS THREE DISCRETE, ELECTRICALLY ISOLATED LOOPS

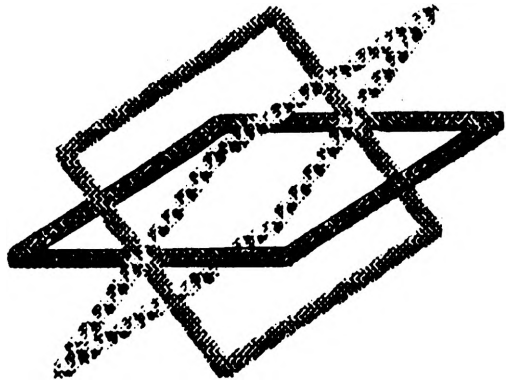

FIGURE 4

STEINMETZ CIRCUIT MODEL FOR THE INDUCTION MOTOR
(ONE PHASE)

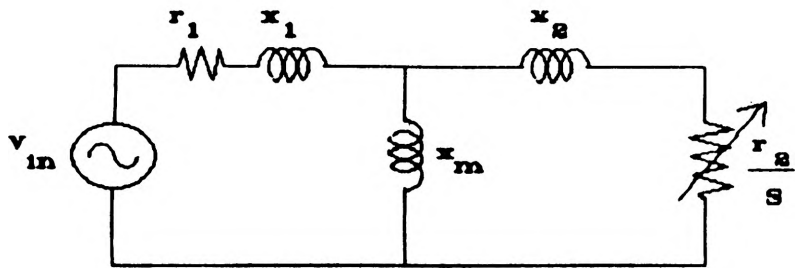

FIGURE 5a

THEVININ EQUIVALENT CIRCUIT

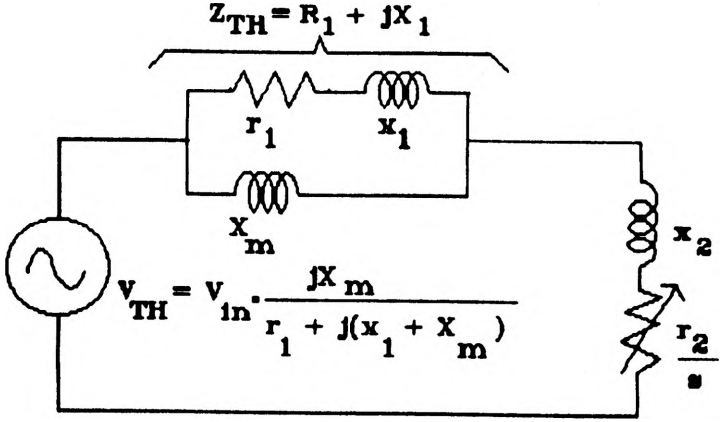

FIGURE 5b

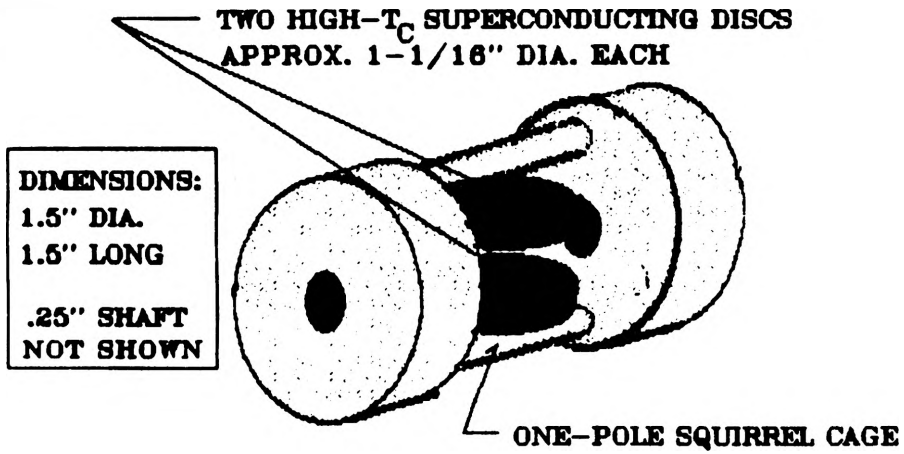

SQUIRREL CAGE AND SUPERCONDUCTING DISCS ENCASED IN LAMINATED IRON CORE AS IN FIGURE 1

FIGURE 6--SUPERCONDUCTING ROTOR

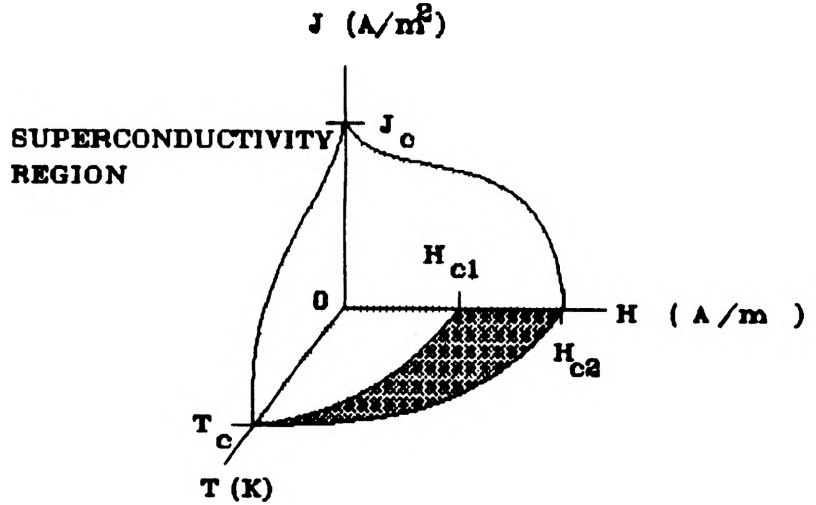

PLAID AREA REPRESENTS FIELD STRENGTHS AT WHICH FLUX PINNING OCCURS.

FIGURE 7

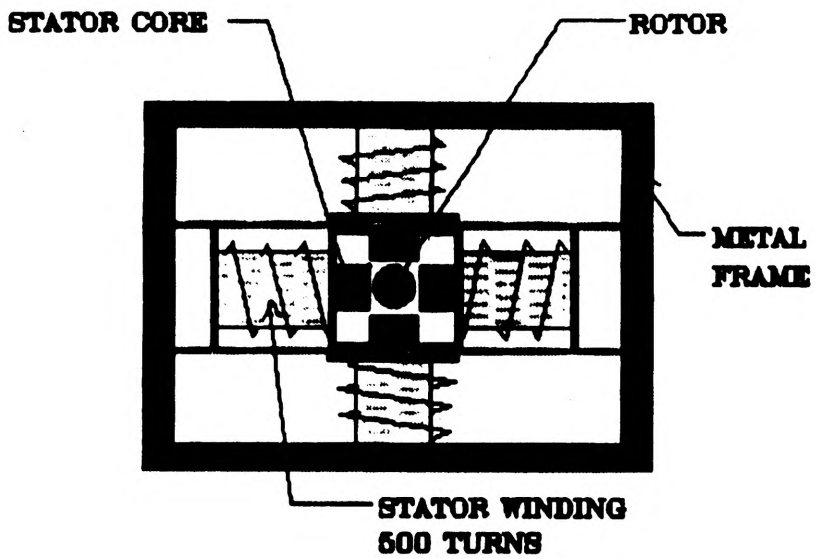

FIGURE 8--MOTOR LAYOUT

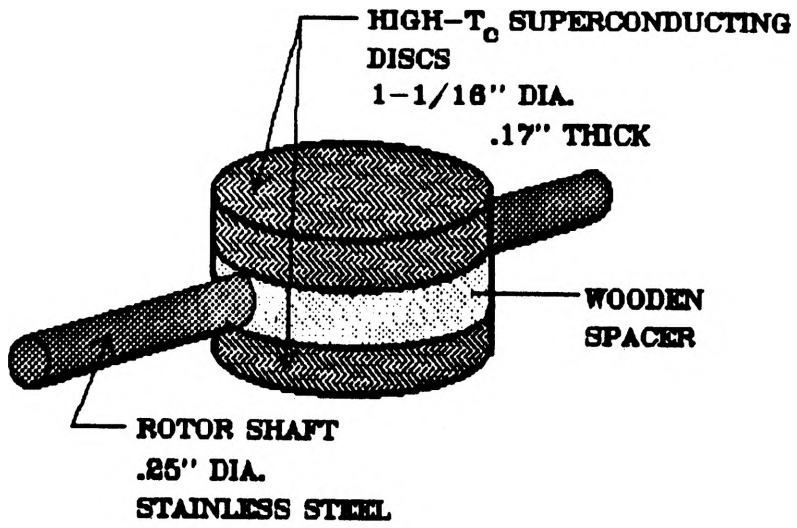

FIGURE 9--EARLY ROTOR DESIGN

TACHOMETER

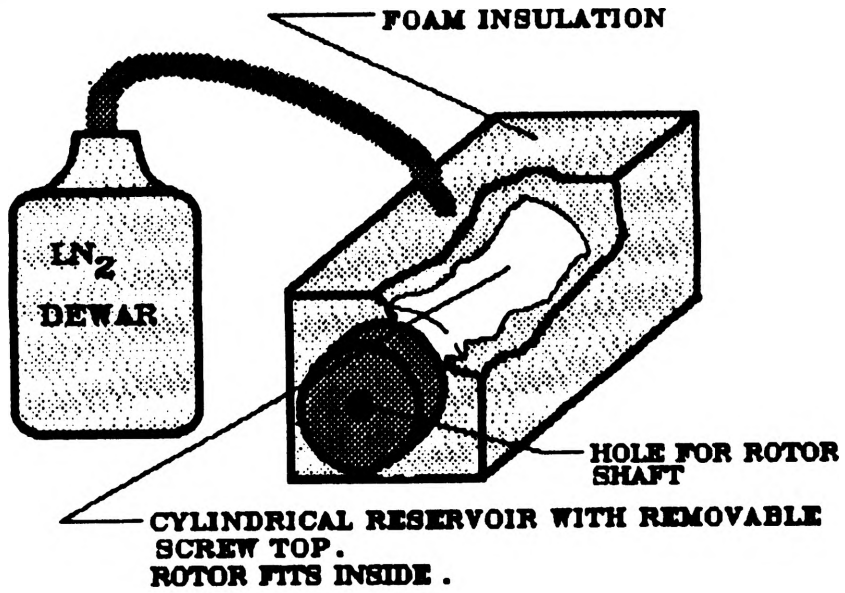

FIGURE 10: LN_2 COOLING SYSTEM

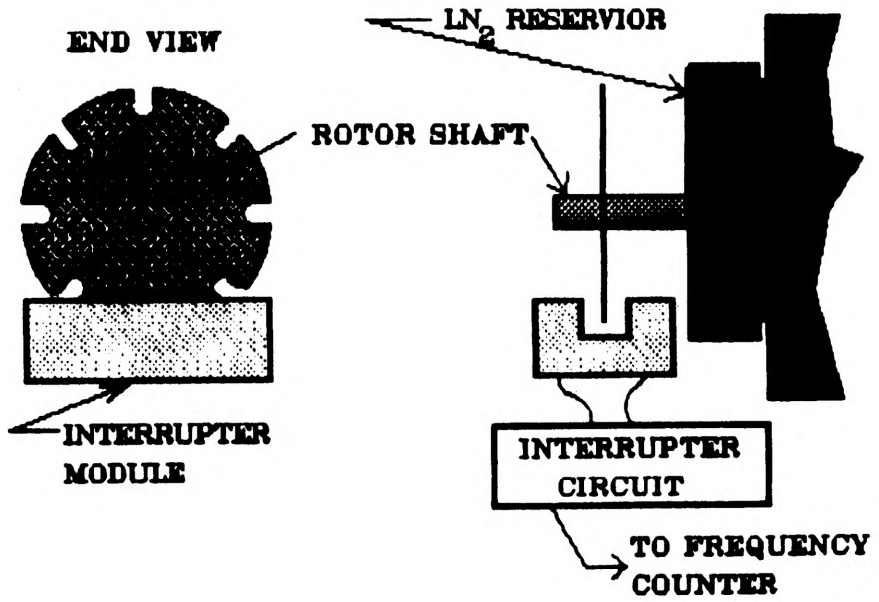

FIGURE 11

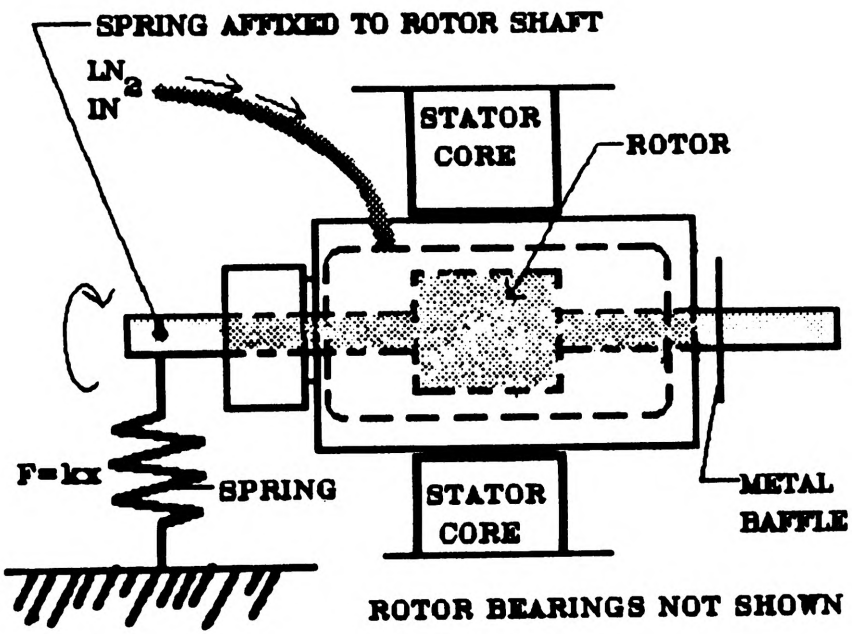

FIGURE 12
MEASUREMENT OF STATIC TORQUE

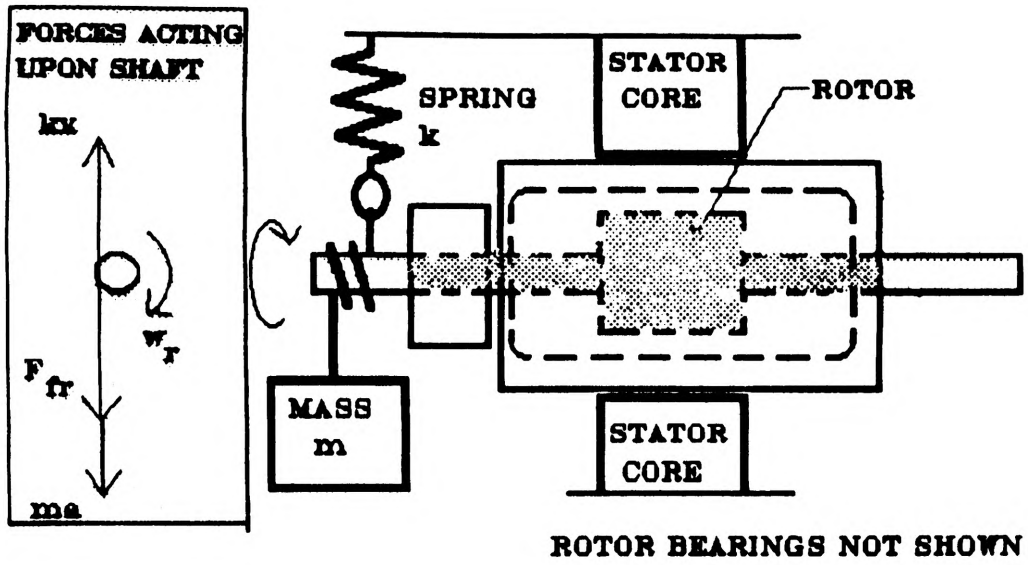

FIGURE 13
MEASUREMENT OF DYNAMIC TORQUE

APPENDIX ONE

Derivation of static torque on a conducting ring.

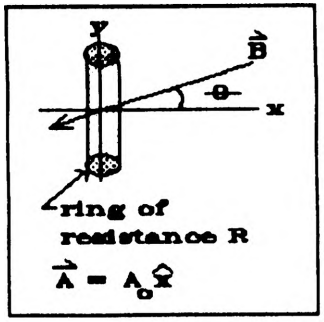

$$\vec{B}(t) = B_o(\hat{x}\cos(wt) + \hat{y}\sin(wt))$$

$$V(t) = -A_o\hat{x}\cdot\frac{d}{dt}B(t) = A_oB_ow(\sin(wt))$$

$$I(t) = V(t)/R$$

$$\vec{M}(t) = I(t)\vec{A} = V(t)\vec{A}/R$$

$$\vec{M}(t) = \hat{x}\frac{B_oA_o^2w}{R}\sin(wt)$$

$$\vec{\tau}(t) = \vec{M}(t) \times \vec{B}(t) = \hat{x}\frac{B_oA_o^2w}{R}\sin(wt) \times B_o(\hat{x}\cos(wt) + \hat{y}\sin(wt))$$

$$\vec{\tau}(t) = \hat{z}\frac{B_o^2A_o^2w}{R}\sin^2(wt)$$